Supporting Information

The swelling-induced fractionation strategy to mediate cellulose availability and lignin structural integrity

Dong Tian,[*a] Yu Zhang,[a] Tingjiao Wang,[a] Baiheng Jiang,[a] Miao Liu,[a] Li Zhao,[a] Jinguang Hu,[b] and Fei Shen,[*a]

a: College of Environment Science, Sichuan Agricultural University, Chengdu, Sichuan 611130, PR China.

E-mail: dongtian@sicau.edu.cn (D. Tian), fishen@sicau.edu.cn (F. Shen).

b: Department of Chemical and Petroleum Engineering, University of Calgary, 2500 University Dr. NW, Calgary, AB T2N 1N4, Canada.

Experimental Section

Alkaline deep eutectic solvents (DES) preparation

Bagasse sample was pretreated by different concentrations of choline hydroxide-ethylene glycol (Ch-Ely) and choline hydroxide-urea (Ch-Ur) DESs, respectively. For the synthesis of these two DESs, the aqueous choline hydroxide was mixed with Ely and Ur at the molar ratio of 1:2 and stirred at 60–70 ℃ until transparent solutions were obtained. The concentrations of the prepared alkaline DES were adjusted to 10%, 20%, 30% and 40% with distilled water.

Alkaline deep eutectic solvents fractionation bagasse

20 g (based on dry weight) bagasse and 400 g aqueous DES solution were conducted at 130 ℃ for 3 h. The reaction mixtures were then cooled to 80 ℃, after which 100 mL of 50% (by volume) ethanol/water solution was added to facilitate the filtration. The resulting cellulose-rich substrates were obtained by washing twice with hot water of 200 mL to remove the residual DESs and lignin. The collected DES filtrate was sequentially precipitated by hydrochloric acid and ethanol to gain the LCCs and xylan fractions. The obtained LCCs and xylan were freeze-dried and stored in a desiccator for further use.

Characterization

Enzymatic accessibility assessment of cellulose fractions.

The chemical composition of the obtained products were determined by the Klason protocol according to TAPPI Standard Method T-222.[1] X-ray diffraction patterns (XRD) of bagasse and cellulose solids were obtained on a Rigaku Ultima IV in Japan using a scanning range of 5−80° and a speed of 5° min^{-1}. The crystallinity index (CrI) of the sample was calculated based on Segal's method.[2] The degree of polymerization (DP) of cellulose solid was obtained based on its intrinsic viscosity values. Briefly, the lignin residues in cellulose solids were first removed with mixed solution of sodium chlorite and acetic acid, and then the solid substrates were dissolved in the copper ethylenediamine solution using an Ubbelohde viscometer according to ASTM D1795.28.[3] Water retention values (WRV) of bagasse and cellulose-rich solids were evaluated by TAPPI-256.[4] Enzymatic hydrolyses of the original bagasse and cellulose-rich materials were performed with a solid loading of 5% and a cellulase (Cellic CTec2) loading of 20 mg g^{-1} in sodium acetate buffer (50 mM, pH 4.8). Then, the mixtures were incubated at 50 °C with 150 rpm for 96 h in a benchtop orbital shaker (ZWYR-2102C Shanghai, China). In the specific time points, 500 μL of hydrolysate was taken in the specific time and incubated on a 105 °C hot plate for 10 min to inactivate the cellulase. After that, the glucose supernatant was collected by centrifuging the solution, which was analyzed by high-performance liquid chromatography (HPLC).

LCC and xylan characterization

The ^{13}C and 2D-HSQC NMR were recorded using a Bruker AVII 600 MHz spectrometer. 100 mg freeze-dried samples were dissolved in 0.7 mL DMSO-d_6, and 0.1 mL Cr (III) acetylacetone (10 μmol mL^{-1}, DMSO-d_6) was added to the mixed solution to completely relax all nuclei. The configuration solution was then transferred to a 5 mm NMR tube. Then NMR were analyzed using MestReNova9 software and compared with the literature.[5] The subunit contents and chemical linkage contents of LCCs were calculated as follows.

$$I_X\% = I_X/(0.5I_{S_{2,6}} + I_{G_2} + 0.5I_{H_{2,6}})\ (1)$$

where I represented the integration of the corresponding signal peak in the 2D-HSQC spectra.

The phenolic hydroxyl content in LCC was determined using the Folin-Ciocalteu method as described in the literature[6]. Thermogravimetric analysis (TGA) was conducted on a thermos gravimetric analyzer (NETZSCH TG 209 F1, Germany). The sample was heated at a rate of 10 °C min^{-1}, and the temperature ranged from room temperature to 800°C under a nitrogen atmosphere.

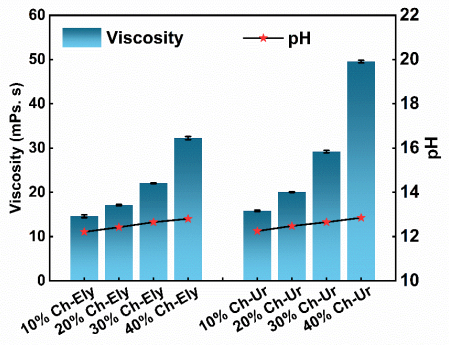

Fig. S1. Physical properties of ChOH-based alkaline DES.

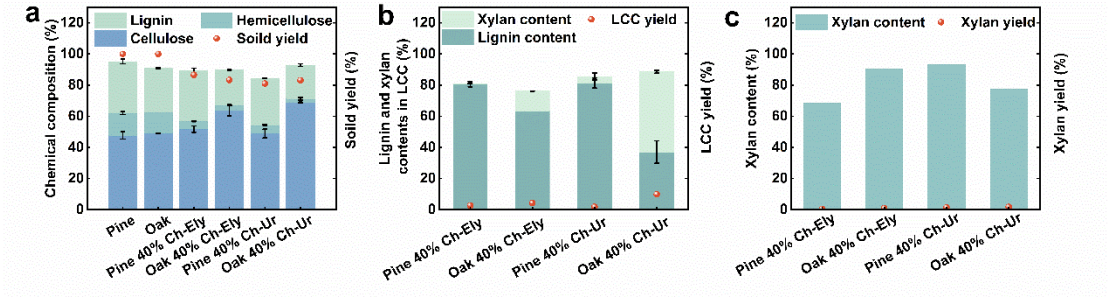

Fig. S2 (a) Chemical composition and solid recovery of bagasse. (b) Chemical compositions and yields of LCC fraction. (c) Purity and yields of xylan fraction. (Reaction conditions were 40% Ch-Ely and 40% Ch-Ur at 130°C for 3h.)

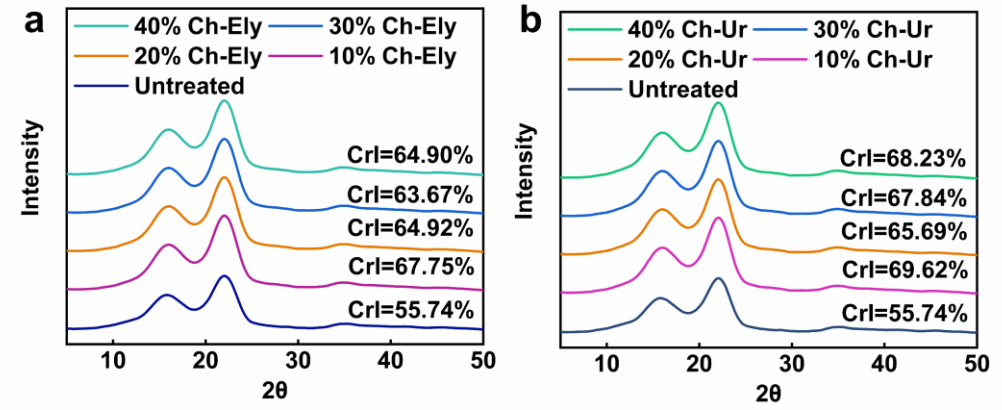

Fig. S3 X-ray diffraction patterns of cellulose fractions pretreated with (a) ChOH-Ethylene glycol and (b) ChOH-Urea, respectively.

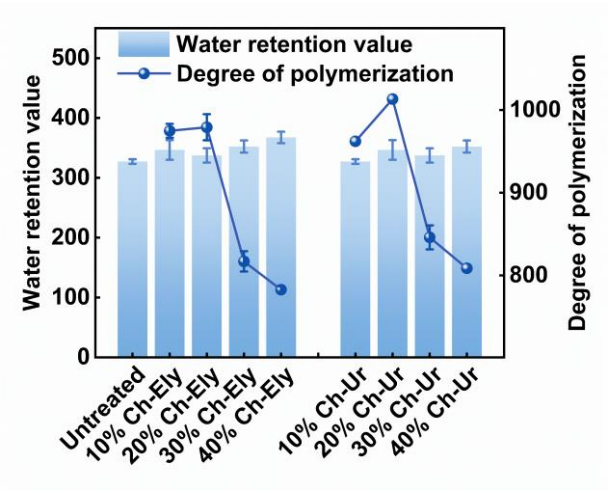

Fig. S4 Water retention value and degree of polymerization of untreated and pretreated samples

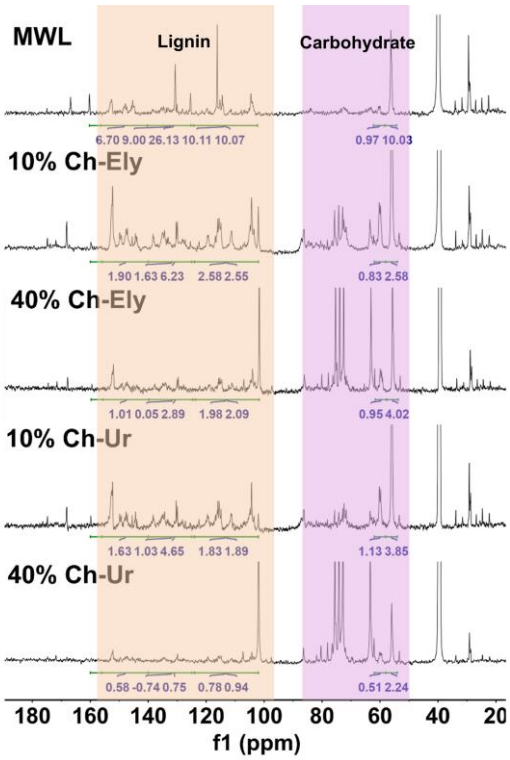

Fig. S5 LCC semi-quantitative ^{13}C NMR.

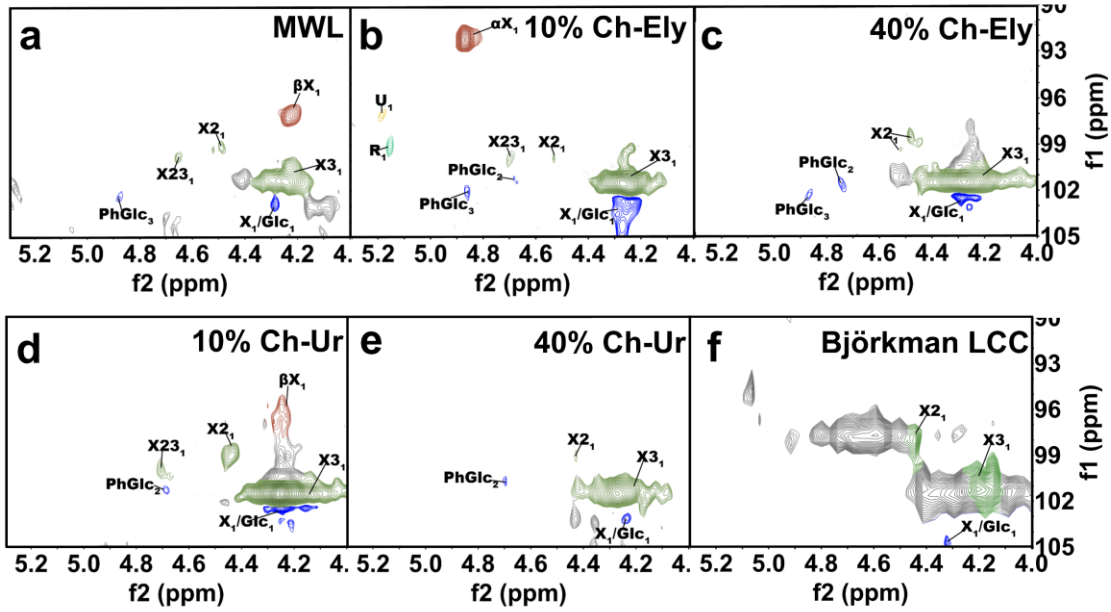

Fig S6 Partially amplified signals, PhGlc (δC/δH 105–100/5.5–4.5 ppm) for different LCCs in the HSQC NMR spectra, (a) MWL, (b) 10% Ch-Ely, (c) 40% Ch-Ely, (d) 10% Ch-Ur, (e) 40% Ch-Ur. (f) Björkman LCC.

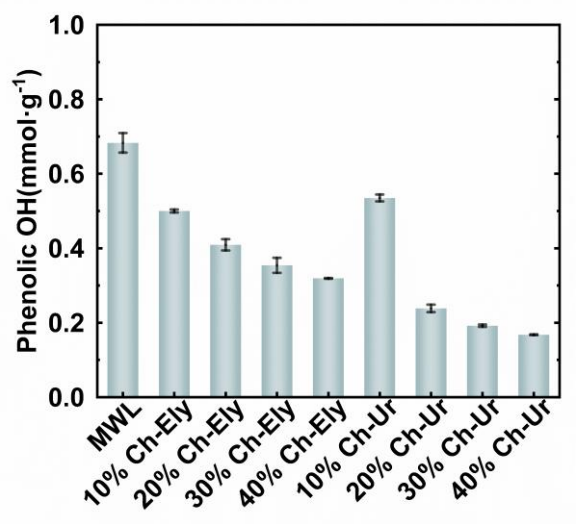

Fig. S7 Phenolic hydroxyl group content of LCC and MWL calculated by Folin-Ciocalteu method.

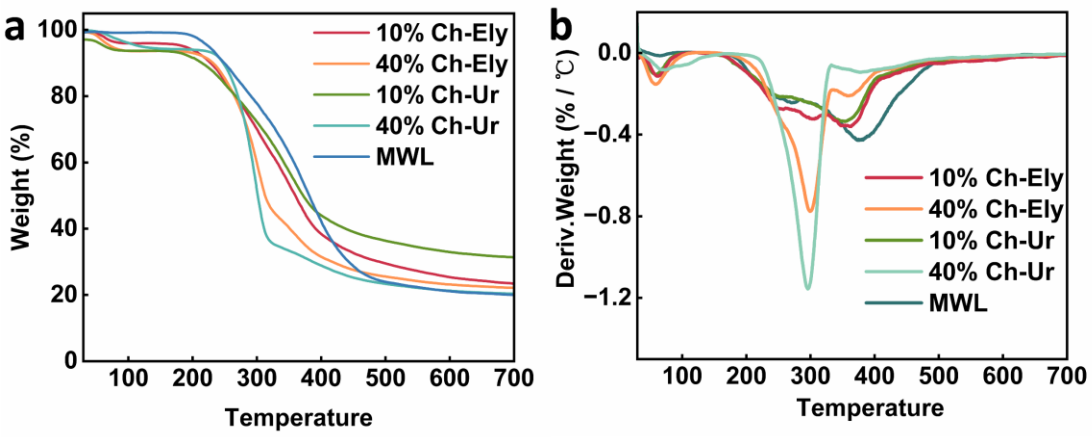

Fig. S8 (a) Typical thermogravimetric analysis (TGA) curves. (b) Differential thermogravimetric (DTG) curves.

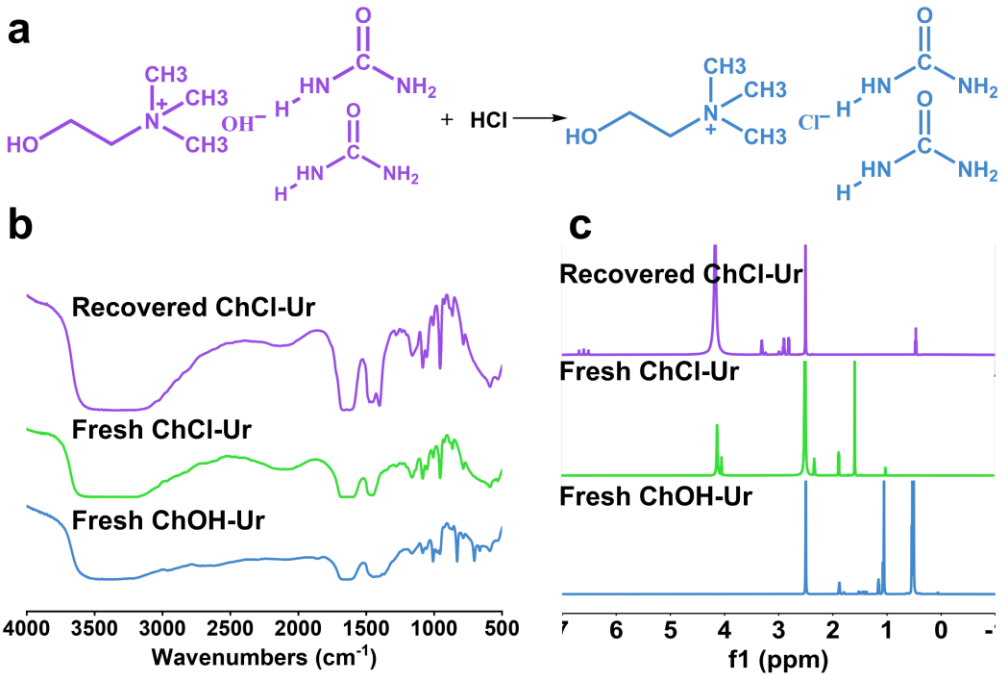

Fig. S9 (a) DES structure change after LCC separation, (b)FTIR and (c) ^{1}H NMR spectra of fresh ChOH-Ur, recovered ChCl-Ur and fresh ChCl-Ur.

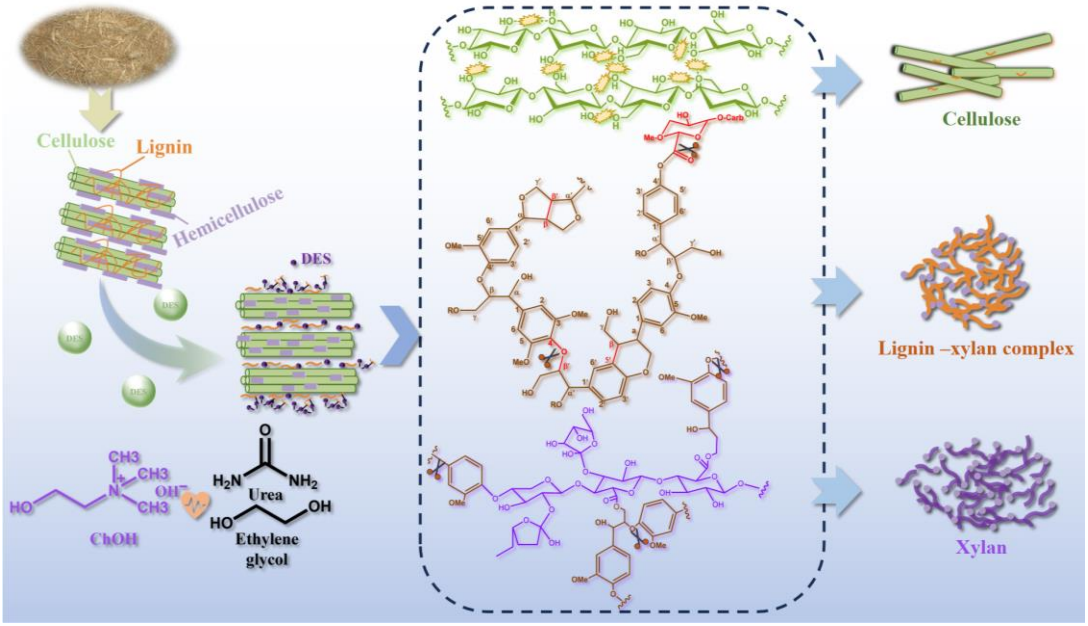

Fig. S10 mechanism of the tailored swelling-induced fractionation lignocellulose strategy.

Table. S1 HPLC raw data for substrate composition analysis. The chemical composition was determined according to the Klason protocol (TAPPI stan‐dard method T-222).

Untreated-1						
Time	Peak area	Peak height	Peak width	Symmetry factor	Peak area %	Type
9.908	28000.7	1557.7	0.2788	0.888	1.058	VB R
11.123	87506.9	4641.1	0.2934	0.829	3.308	BV
11.697	45789.6	2388.4	0.3014	0.833	1.731	VB
Untreated-2						
Time	Peak area	Peak height	Peak width	Symmetry factor	Peak area %	Type
9.908	29114.1	1615.4	0.2794	0.886	1.085	VB R
11.124	88226.5	4770.2	0.2914	0.794	3.288	BV
11.696	47900.1	2470.2	0.3018	0.822	1.785	VV R
40% ChOH-1						
Time	Peak area	Peak height	Peak width	Symmetry factor	Peak area %	Type
10.268	23760.09	871	0.3677	0.835	0.677	VBAE
11.425	86705	5913.6	0.3878	0.864	4.613	MM
12.967	3282	24	0.3166	0.29	0.019	BB
40% ChOH-2						
Time	Peak area	Peak height	Peak width	Symmetry factor	Peak area %	Type
10.222	22229	806.3	0.3463	0.806	0.65	VBAE
11.35	82933	43.9	0.2359	1.414	0.023	BB
11.968	2156	2023.1	0.348	0.805	1.555	MM
10% Ch-Ely-1						
Time	Peak area	Peak height	Peak width	Symmetry factor	Peak area %	Type
9.917	29041.4	1579.3	0.2858	0.837	1.166	VB R
11.135	146889	7844.2	0.2941	0.79	5.899	BV
11.705	31116.5	1601.6	0.3001	0.805	1.25	VV R
10% Ch-Ely-2						
Time	Peak area	Peak height	Peak width	Symmetry factor	Peak area %	Type
9.917	29913.5	1611	0.2861	0.839	1.111	VV R
11.135	131393.3	7101	0.2915	0.787	4.881	BV
11.708	61397.6	3154.2	0.3027	0.819	2.281	VV R

Continued Table

20% Ch-Ely-1						
Time	Peak area	Peak height	Peak width	Symmetry factor	Peak area %	Type
9.918	29028.8	1562.1	0.2865	0.841	1.084	VV R
11.136	138721.1	7500.9	0.2892	0.785	5.18	BV
11.709	56142.2	2874.5	0.3035	0.813	2.096	VV R
20% Ch-Ely-2						
Time	Peak area	Peak height	Peak width	Symmetry factor	Peak area %	Type
9.918	29039.2	1566.2	0.2858	0.84	1.083	VV R
11.137	139195	7525.4	0.2914	0.785	5.193	BV
11.71	54807.3	2851.7	0.2998	0.838	2.045	VB
30% Ch-Ely-1						
Time	Peak area	Peak height	Peak width	Symmetry factor	Peak area %	Type
9.917	29335.4	1573.1	0.2871	0.819	1.073	VV R
11.135	150469.3	8112.6	0.292	0.782	5.503	BV
11.708	51681.4	2650.9	0.3031	0.817	1.89	VV R
30% Ch-Ely-2						
Time	Peak area	Peak height	Peak width	Symmetry factor	Peak area %	Type
9.915	29143.2	1591	0.285	0.829	1.075	VV R
11.133	148724.5	8022.8	0.2919	0.783	5.486	BV
11.706	50876	2606.4	0.3033	0.813	1.877	VV R
40% Ch-Ely-1						
Time	Peak area	Peak height	Peak width	Symmetry factor	Peak area %	Type
9.915	28854.3	1582.8	0.2809	0.789	0.823	VV R
11.133	154317.9	8333.1	0.2895	0.78	4.403	BV
11.706	45072.4	2309.3	0.3012	0.81	1.286	VV R
40% Ch-Ely-2						
Time	Peak area	Peak height	Peak width	Symmetry factor	Peak area %	Type
9.911	29920.1	1626.3	0.2859	0.798	1.11	VV R
11.129	153642.3	8291.7	0.2918	0.782	5.7	BV
11.701	45015.9	2341.8	0.2999	0.834	1.67	VB

Continued Table

10% Ch-Ur-1

Time	Peak area	Peak height	Peak width	Symmetry factor	Peak area %	Type
9.909	30057.7	1615.5	0.2862	0.811	1.125	VB R
11.125	150534.5	8124.1	0.2918	0.781	5.636	BV
11.697	49686.4	2546.1	0.3011	0.817	1.86	VV R

10% Ch-Ur-2

Time	Peak area	Peak height	Peak width	Symmetry factor	Peak area %	Type
9.907	28761.2	1565.2	0.2857	0.83	1.054	VV R
11.123	152543.8	8245.9	0.2914	0.781	5.59	BV
11.695	50640	2597.3	0.3031	0.813	1.856	VV R

20% Ch-Ur-1

Time	Peak area	Peak height	Peak width	Symmetry factor	Peak area %	Type
9.907	28525.6	1553.9	0.2855	0.855	1.044	VV R
11.124	133321.7	7216.6	0.2911	0.787	4.877	BV
11.697	61423.1	3150.7	0.303	0.815	2.247	VV R

20% Ch-Ur-2

Time	Peak area	Peak height	Peak width	Symmetry factor	Peak area %	Type
9.905	29410.9	1592	0.2847	0.848	1.095	VV R
11.121	131487.1	7108.8	0.2892	0.783	4.895	BV
11.694	60665	3113.6	0.3029	0.815	2.258	VV R

30% Ch-Ur-1

Time	Peak area	Peak height	Peak width	Symmetry factor	Peak area %	Type
9.905	28962	1564.3	0.2851	0.808	1.051	VB R
11.122	161046.5	8660	0.2926	0.777	5.845	BV
11.693	40440.1	2066.3	0.3018	0.804	1.468	VV R

30% Ch-Ur-2

Time	Peak area	Peak height	Peak width	Symmetry factor	Peak area %	Type
9.908	28758.7	1553.1	0.2873	0.811	1.061	VV R
11.124	162040.7	8711.1	0.2926	0.779	5.979	BV
11.695	40513.1	2069.6	0.3018	0.805	1.495	VV R

Continued Table

40% Ch-Ur-1						
Time	Peak area	Peak height	Peak width	Symmetry factor	Peak area %	Type
9.902	28602.2	1547.7	0.2847	0.787	1.058	VB R
11.117	175507.6	9273.8	0.2964	0.748	6.489	BV R
11.688	29959	1616.4	0.2897	0.689	1.108	VV E
40% Ch-Ur-2						
Time	Peak area	Peak height	Peak width	Symmetry factor	Peak area %	Type
9.905	29442.9	1587.6	0.2855	0.749	0.844	VV R
11.12	175158.2	9141.7	0.297	0.78	5.019	BV R
11.693	28104.8	1538.8	0.2865	0.713	0.805	VB E

Reference

1. R. P. Chandra, K. Gourlay, C.-S. Kim and J. N. Saddler, *ACS Sustainable Chemistry & Engineering*, 2015, **3**, 986-991.
2. Y. Zhang, Q. Hou, W. Xu, M. Qin, Y. Fu, Z. Wang, S. Willför and C. Xu, *Industrial Crops and Products*, 2017, **108**, 864-871.
3. X.-J. Shen, T. Chen, H.-M. Wang, Q. Mei, F. Yue, S. Sun, J.-L. Wen, T.-Q. Yuan and R.-C. Sun, *ACS sustainable chemistry & engineering*, 2019, **8**, 2130-2137.
4. F. Shen, D. Tian, G. Yang, S. Deng, F. Shen, J. He, Y. Zhu, C. Huang and J. Hu, *ACS Sustainable Chemistry & Engineering*, 2020, **8**, 11253-11262.
5. F. Shen, S. Wu, M. Huang, L. Zhao, J. He, Y. Zhang, S. Deng, J. Hu, D. Tian and F. Shen, *Green Chemistry*, 2022, **24**, 5242-5254.
6. M. Pérez, I. Dominguez-López and R. M. Lamuela-Raventós, *Journal of Agricultural and Food Chemistry*, 2023, **71**, 17543-17553.